HHS Public Access

Author manuscript

Med Chem. Author manuscript; available in PMC 2015 September 14.

Published in final edited form as:

Med Chem. 2011 September ; 7(5): 389–394.

^{89}Zr Radiochemistry for PET

G.W. Severin, **J.W. Engle**, **R.J. Nickles**, and **T.E. Barnhart**

Medical Physics Department, University of Wisconsin-Madison, Madison WI, 53705

Abstract

The positron emitting isotope ^{89}Zr is an ideal radiolabel for PET imaging of monoclonal antibodies (mAbs). This article reviews the chemistry and physics involved in production, separation, chelation, and labeling of ^{89}Zr mAbs.

I. Introduction

An emerging application of positron emission tomography (PET), termed immuno-PET [1], uses the cancer targeting capabilities of monoclonal antibodies (mAbs) to generate tomographic data. This PET data quantifies the expression of the target protein or gene, enabling the researcher to characterize tumor conditions and responses to treatment. In cases where the antibody itself acts as an inhibitor to tumor function, immuno-PET determines binding and exchange constants for drug action. Similarly, when the mAb is employed in radio-immuno-therapy (RIT), the PET scan provides an accurate picture of dose distribution and targeting effectiveness [2].

Many researchers currently use ^{89}Zr as the radiolabel for immuno-pet. In general, after separation from cyclotron target material, they attach ^{89}Zr is to mAbs through conjugation and chelation, enabling the composite molecule, rather than zirconium-specific chemistry, to target the antigen.

The concerns of radiometal labeling using other isotopes apply equally to radio-zirconium syntheses. In brief, metal impurities increase the number of chelation sites occupied by stable atoms, so no-carrier-added ^{89}Zr chemistry requires stringent attention to reagent purity and separation efficacy. The chelant must also remain bound to the mAb and the ^{89}Zr *in vivo* without impairing the immunoreactivity or specificity of the mAb.

The chemical and physical characteristics of ^{89}Zr justify the effort expended to control these variables. The 3.27 day half-life matches mAb pharmacokinetics in tumors (2–4 d) [3]. Production of ^{89}Zr via cyclotron irradiation uses an unenriched, metal Yttrium target. Furthermore, the common bifunctional chelant for ^{89}Zr is desferrioxamine B (Df), a biologically produced siderophore that is sold under the trade name Desferal (Novartis) for chelation therapy in humans [4]. Zr(IV) has one of the highest affinities of all metals for this chelant, and remains bound *in vivo* [5]. Finally, three papers [6–8] and a recent protocol [9] constitute a veritable instruction manual for the production of a reactive ^{89}Zr radiolabel in a matter of hours.

The increasing availability of ^{89}Zr has resulted in a sizeable amount of work with the isotope, fostering a growing body of literature. This article reviews the chemistry and physics that researchers employ in ^{89}Zr immuno-PET to go from cyclotron bombardment to tomographic imaging.

II. ^{89}Zr Physics

^{89}Zr is a neutron deficient isotope of Zirconium with 49 neutrons and 40 protons, and it decays with a half-life of 3.27 days to ^{89}Y. The decay proceeds via electron capture (77%), and positron emission (23%). Both modes of decay lead primarily (99%) to a 9/2+ state in ^{89}Y, which de-excites through M4 emission of a 909 keV gamma ray to the 1/2- ground state.

Therefore the important decay radiations are the 511 keV γ's from positron annihilation, the 909 keV γ from the ^{89m}Y de-excitation, continuum positrons (23% endpoint = 902 keV), internal conversion electrons from the M4 transition (0.8%), and Auger electrons. Figure [1] shows a simplified level scheme for ^{89}Zr decay [10].

III. Cyclotron Production of ^{89}Zr

Typically, ^{89}Zr is created by proton bombardment of ^{89}Y. The isotopic abundance of the natural target is 100%, making production affordable, and alleviating the need for complicated target recycling procedures. Yttrium foils (99.9%, Goodfellows) can be purchased from distributors in various thicknesses. Yttrium melts at 1526°C, and is not highly reactive. Besides foils, several groups use sputtered targets with gold or copper backings to improve heat dissipation during irradiation. Additionally, powder targets of both yttrium metal and Y_2O_3 appear in the literature. The final choice of target type depends upon cooling capabilities of the cyclotron and the amount of ^{89}Zr desired.

Omara *et al* (2009) measured the cross-sections for production of ^{88}Zr, ^{88}Y, and ^{89}Zr from proton irradiation of metal yttrium [11]. They conclude that the optimum energy for proton bombardment is 14 MeV, with a thick-target short-irradiation yield of 58 MBq/μAh. Above the threshold incident energy of 13.1 MeV, proton irradiation also produces the isotopic impurity ^{88}Zr by (p,2n). The 83.4 day half-life of ^{88}Zr decay creates problematic dosimetry which is exacerbated by the 106 day half-life of its daughter, ^{88}Y.

Zweit *et al.* used the ^{89}Y(d,2n)^{89}Zr reaction to reduce production of contaminant ^{88}Zr [12]. The threshold for ^{89}Zr production with a deuteron beam is 5.6 MeV, whereas it is 15.5 MeV for ^{88}Zr production. Figure 2 shows the estimated thick target yields of ^{88,89}Zr for both proton and deuteron bombardment as a function of projectile energy. Based upon the characteristics of the cyclotron being used, the plot shows which projectile is most expedient to maximize ^{89}Zr production while limiting production of ^{88}Zr.

IV. Separation Chemistry

Several groups have reported methods for separating ^{89}Zr embedded in the metal Yttrium target. Most begin with dissolution in strong hydrochloric acid. From here, methods diverge,

utilizing solvent extraction [15], anion exchange chromatography [12], or weak cation exchange chromatography [16].

The most widely used of these procedures is the weak cation exchange method using a hydroxamic acid resin. Meijs *et al* performed the first separations of ^{89}Zr from Yttrium with a custom hydroxamic acid resin, and developed their method by separating ^{88}Zr(IV) from ^{88}Y(III) and ^{59}Fe(III), eluting the desired product with oxalic acid [16]. Separations reported since this time use this method exclusively.

Hersheid *et al.* (1983) report original synthesis of the resin for use in a ^{52}Fe/^{52m}Mn generator [17]. Figure 3 depicts the chemical mechanism as described in [7]. The synthesis begins with the formation of an ester bond from the carboxyl group on the resin to the central carbon in the carbodiimide group on 1-Ethyl-3-(3-dimethylaminopropyl)carbodiimide (EDAC). The ester bond is subject to nucleophillic attack by terminal amines and alcohols, in addition to being prone to hydrolysis. To limit reactivity, tetrafluorophenol (TFP) is added, transferring the ester bond to the TFP hydroxyl group. In this reaction an EDAC-derived alcohol leaving group rapidly tautomerizes to the urea derivative, limiting the reverse reaction.

The TFP ester is stable to attack from alcohols and hydrolysis but still reacts with terminal amines. Hydroxylamine hydrochloride displaces TFP to form the functionalized hydroxamic acid resin. Once the resin is functionalized it is stable for more than one year [7].

To perform the Yttrium-Zirconium separation, a column is packed with the resin and equilibrated with 2M hydrochloric acid. Then the dissolved Yttrium target is loaded onto the resin in <2M HCl and washed with 2M HCl and water. Elution is performed with small volumes of 1M oxalic acid. A typical separation uses 100mg of resin to collect several hundred MBq of ^{89}Zr from about 500 mg of Yttrium. Under these conditions, greater than 70% of the ^{89}Zr is eluted in 2 ml of oxalic acid [7].

In the original paper by Meijs, the authors express concern over the ability of Zirconium in oxalate complexes to trans-chelate to Df. Since then Holland *et al.* have shown that chelation efficacy is not impaired by oxalate. They also describe a method for removing the oxalate and replacing it with chloride on an anion exchange column[7]. Work by Verel suggests that the chloride form is undesirable due to hypochlorite formation from radiolysis [3]. The protocol describing general mAbs labeling techniques calls for the oxalate form of ^{89}Zr [9].

V. Selective Chelation with Desferrioxamine B and its Derivatives

The most successful Zr(IV) chelant is desferrioxamine B (Df). Figure 4 shows the bare Df molecule (A) along with the Zr-Df compound and the stable structure as determined by a density functional theory (DFT) calculation (B) [18]. The bacteria strain *Streptomyces pilosus* naturally creates Df as an Fe(III) scavenging siderophore [19]. The FDA has approved Df for drug use to treat acute iron intoxification (Desferal, NDA:016267) and Novartis produces it as a pharmaceutical. The fact that Df is considered safe for humans in

bare and metal-complexed forms alleviates concerns that it may be harmful if it dissociates from its tagged mAb.

Although there is no published value for the stability constant of the conjugated Zr-Df pair, Holland suggests that Zr(IV)-Df is more stable than the iron-Df complex [7]. The stability constant for Fe(III)-Df is over 10^{31} [19]. A study by Baroncelli shows that Zr(IV) complexed to a single hydroxamate group, has a stability constant greater than 10^{12}, this grows to more than 10^{24} when complexed to two hydroxamates [20]. Since deprotonated Df is a string of three hydroxamate groups, the qualitative stability of Df-Zr is assumed. Additionally, Holland has shown through DFT calculations that the Zr-Df compound is thermodynamically stable and that solvating water molecules increase stability [18]. Further, a paper by Takagai shows that Df is highly selective of Zr(IV) (compared to other high valence metals) when the Df is immobilized at its amine terminus[21].

Presently, no alternative chelants compete with Df for the clinical radiochemist's attention in the literature. In a 2006 paper, Perk *et al.* attempted to label the mAb Zevalin with ^{89}Zr via chelation to diethyl tetraamine pentacetic acid (DTPA), and achieved less than 0.1% labeling efficiency [22]. This is despite the fact that DTPA forms stable complexes with Zr[7]. In an earlier work, Meijs compared the *in vitro* stabilities of Zr-Df and Zr-DTPA to show that the Zr-DTPA complex undergoes 20% demetalation in 24 hours in human serum [5]. Zr-Df, on the other hand, remains 99% intact after seven days of incubation[7].

The phenomenal stability of the Zr-Df complex is important because PET imaging depends on *in vivo* stability for quantification of tracer kinetics. In order to understand the effects of 89Zr-Df-mAb dissociation, Holland *et al.* investigated the *in vivo* characteristics of ^{89}Zr-chloride, oxalate, and Df. They showed that un-chelated Zr(IV) from $ZrCl_4$ accumulates in the liver, while the Zr-oxalate complex is taken up in bone[18]. Df-conjugated Zr, however, is expelled quickly via the kidneys with a time constant of about 300 seconds. Meijs *et al.* (1996) report similar results in an earlier study [25]. These results indicate that biodistribution studies of ^{89}Zr-Df-mAbs are adversely affected by de-metallation but not by dissociation of the chelant from the antibody.

In terms of functionalization, the terminal amine on Df is the locus of modification. Two derivatives of Df are commonly used for labeling: the carboxylated form, Df-N-suc, and an isothiocyanato-benzyl form called Df-Bz-NCS. Both of these compounds target amine groups on lysine residues for conjugation to mAbs. Hersheid *et al.* describe the procedure for modification to the carboxylate form [23], and the method for Df-Bz-NCS production is described by Perk *et al.* [8]. Both forms are available commercially.

Tinianow *et al.* developed three Df derivatives with functional groups that are reactive with the thiol groups on cysteine residues [24]. They used modified mAbs with an artificially placed cysteine residue outside of the active-site for attaching the chelant. While successful, this method is not generalizeable. With the other two Df compounds listed above, any antibody can be labeled, whereas thiol targeting compounds require an engineered mAb (termed THIOMAB).

VI. Labeling Antibodies

One of the first published methods for attaching Df to proteins appears in reference [25]. The authors premodified the lysine residues on bovine serum albumin with maleimide groups through reaction with succinimidyl 4-(N maleimidomethyl)cyclohexane-1-carboxylate. They also synthesized a Df derivative, SATA-Df, by reacting Df with N-succinimidyl S-acetylthioactetate. The maleimide modified lysine groups react with the thioester in SATA-Df creating a stable thiolether bond, linking the Df to the protein. Labeling yields for this method were approximately 90% after 1 hour of incubation with Zr(IV) oxalate.

Since that initial labeling, two easily followed procedures have been published which do not involve pre-modification of the lysine residues. The first method, used initially by Verel *et al.* [3], involves six steps. They start with Df, and modify the amine group using succinic anhydride to create a terminal carboxyl group (Df-N-suc). Then they protect the Df through complexation with Fe(III) and esterify it to TFP in the same manner as stated above for creation of the hydroxamate resin. This TFP ester reacts with the amine group on mAb lysine residues to create the peptide bond. Transmetallation of the Fe(III) to EDTA deprotects the chelant. Finally, they add ^{89}Zr oxalate and incubate for 30 minutes to make the final [^{89}Zr]mAb. This procedure reproducibly conjugated one Df per mAb and chelated Zr(IV) from the oxalate with 80% efficiency.

An alternative lysine linkage method involves the direct reaction of the isothiocyanate group on Df-Bz-NCS to the amine group in lysine, forming a thiourea bond [8]. When introducing this method, the authors reported similar yields to the six-step method, with no loss of *in vitro* stability.

The paper by Tinianow *et al.* describes the reactions for conjugating the cysteine linking Df derivatives. Briefly, they reacted the three modified Df molecules with mAbs' engineered thiol groups. All three Df molecules form thioethers with the cysteine residues, and their conjugated stabilities compare favorably with lysine-linked counterparts. The group also conducted a study comparing the number of conjugated Df molecules per antibody for their method, and those of the lysine linkers mentioned above. They found that all methods yield between 1.6 and 2.4 Df conjugates per mAb [24].

VIII. Application

Once the labeling is complete, it is no longer necessary to consider zirconium chemistry. That is, the only remaining chemistry is that of the antibody-antigen matching. The scope of those combinations will not be covered here, simply because the interactions are not unique to zirconium. However, in the interest of highlighting what researchers have accomplished with ^{89}Zr, the following paragraphs survey exemplary ^{89}Zr-mAbs studies.

Over the past five years, researchers at Vrije University (Amsterdam) developed ^{89}Zr-mAbs as imaging agents for RIT [2,22,26]. Conventional RIT uses ^{90}Y in high doses on chimeral mAbs. However, ^{90}Y only emits approximately 32 positrons per million decays, making it a challenging nuclide for PET imaging[27]. As an alternative, Perk *et al.* used a combination

of ^{90}Y- and ^{89}Zr- labeled zevalin (ibritumomab, a CD20 targeting mAb) and performed PET scans to quantify dose delivery [22].

Many researchers use ^{89}Zr labeling with small animal immuno-PET to assess the targeting of mAbs in preclinical studies. The Vrije group labeled cetuximab, an epidermal growth factor receptor (EGFR) targeting mAb, with ^{89}Zr in two studies and showed that EGFR expression was not consistent with cetuximab uptake *in vivo*[26,28]. Another study was undertaken by many of the same authors to show the correlation of bevacizumab, a vascular endothelial growth factor (VEGF) targeting mAb, uptake to VEGF expression [29]. This was followed up by a report utilizing [^{89}Zr]bevacizumab to asses angiogenisis after treatment with HSP90 (heat-shock protein 90) inhibitor NVP-AUY922 [30]. Several other papers report preclinical, small-animal PET with 89Zr [18,24,31–35].

The Vrije group has also administered ^{89}Zr-mAbs clinically. They used [^{89}Zr]U36 (a CD44 targeting mAb), to compare immuno-PET to FDG-PET, CT/MRI in locating lymph node metastases in 20 patients with head and neck squamous cell cancers (HNSCC). The results indicate that ^{89}Zr immuno-PET in HNSCC models outperforms the other imaging modalities [36,37]. One other clinical study used an anti-HER2 (human epidermal growth factor receptor 2) mAb, trastuzumab, to locate HER2 positive lesions in breast cancer patients[38].

IX. Conclusion

Modern cyclotrons and radiochemistry labs can easily create conditions necessary for expedient, economical production of ^{89}Zr in a chemically useful form. Unenriched, thermodynamically and electrically conductive Yttrium metal foils are ideal targets for medical accelerators, yielding radioisotopically pure product in quantities that can support numerous experiments and clinical procedures. The simplicity of established separation procedures lends them to automation, which will only further increase the use of this potential-laded radioisotope. With irradiation and separation procedures so well established, the task now falls to the biochemist to pursue pharmacokinetic questions underpinned by days-long physiological time courses. The breadth of ^{89}Zr's application to medical imaging science will therefore continue to expand alongside the versatility of modern radio-metal chelation chemistry and the target-specific affinities achieved by synthetic antibodies and other novel ligands.

X. References

1. van Dongen GAMS, Visser GWM, Lub-de Hooge MN, de Vries EG, Perk LR. Immuno-PET: A Navigator in Monoclonal Antibody Development and Applications. The Oncologist. 2007; 12:1379–1389. [PubMed: 18165614]
2. Verel I, Visser GW, van Dongen GA. The promise of immuno-PET in radioimmunotherapy. J Nucl Med. 2005; 46(Suppl 1):164S–171S. [PubMed: 15653665]
3. Verel I, Visser GW, Boellaard R, Stigter-van Walsum M, Snow GB, van Dongen GA. 89Zr immuno-PET: comprehensive procedures for the production of 89Zr-labeled monoclonal antibodies. J Nucl Med. 2003; 44:1271–1281. [PubMed: 12902418]
4. Miller MJ. Syntheses and therapeutic potential of hydroxamic acid based siderophores and analogs. Chemical Reviews. 1989; 89:1563–1579.

5. Meijs WE, Herscheid JD, Haisma HJ, Pinedo HM. Evaluation of desferal as a bifunctional chelating agent for labeling antibodies with Zr-89. Int J Rad Appl Instrum A. 1992; 43:1443–1447. [PubMed: 1334954]
6. Verel I, Visser GW, Boellaard R, Boerman OC, van Eerd J, Snow GB, Lammertsma AA, van Dongen GA. Quantitative 89Zr immuno-PET for in vivo scouting of 90Y-labeled monoclonal antibodies in xenograft-bearing nude mice. J Nucl Med. 2003; 44:1663–1670. [PubMed: 14530484]
7. Holland JP, Sheh Y, Lewis JS. Standardized methods for the production of high specific-activity zirconium-89. Nucl Med Biol. 2009; 36:729–739. [PubMed: 19720285]
8. Perk LR, Vosjan MJ, Visser GW, Budde M, Jurek P, Kiefer GE, van Dongen GA. p-Isothiocyanatobenzyl-desferrioxamine: a new bifunctional chelate for facile radiolabeling of monoclonal antibodies with zirconium-89 for immuno-PET imaging. Eur J Nucl Med Mol Imaging. 2010; 37:250–259. [PubMed: 19763566]
9. Vosjan MJ, Perk LR, Visser GW, Budde M, Jurek P, Kiefer GE, van Dongen GA. Conjugation and radiolabeling of monoclonal antibodies with zirconium-89 for PET imaging using the bifunctional chelate p-isothiocyanatobenzyl-desferrioxamine. Nat Protoc. 2010; 5:739–743. [PubMed: 20360768]
10. Singh B. Nuclear Data Sheets for A = 89. Nuclear Data Sheets. 1998; 85:1–170.
11. Omara HM, Hassan KF, Kandil SA, Hegazy FE, Saleh ZA. Proton induced reactions on 89Y with particular reference to the production of the medically interesting radionuclide 89Zr. Radiochimica Acta. 2009; 97:467–471.
12. Zweit J, Downey S, Sharma HL. Production of no-carrier-added zirconium-89 for positron emission tomography. International Journal of Radiation Applications and Instrumentation. Part A Applied Radiation and Isotopes. 1991; 42:199–201.
13. Wenrong Z, Qingbiao S, Hanlin L, Weixiang Y. Investigation of Y-89(p,n)Zr-89, Y-89(p,2n)Zr-88 and Y-89(p,pn)Y-88 reactions up to 22 MeV. Chinese J of Nuclear Physics (Beijing). 1992; 14:7.
14. La Gamma AM, Nassiff SJ. Excitation Functions for Deuteron-Induced Reactions on 89Y. Radiochimica Acta. 1973; 19:161.
15. Dejesus OT, Nickles RJ. Production and purification of 89Zr, a potential PET antibody label. International Journal of Radiation Applications and Instrumentation. Part A Applied Radiation and Isotopes. 1990; 41:789–790.
16. Meijs WE, Herscheid JDM, Haisma HJ, Wijbrandts R, van Langevelde F, Van Leuffen PJ, Mooy R, Pinedo HM. Production of highly pure no-carrier added 89Zr for the labelling of antibodies with a positron emitter. Applied Radiation and Isotopes. 1994; 45:1143–1147.
17. Herscheid JD, Vos CM, Hoekstra A. Manganese-52m for direct application: a new 52Fe/52mMn generator based on a hydroxamate resin. Int J Appl Radiat Isot. 1983; 34:883–886. [PubMed: 6874114]
18. Holland JP, Divilov V, Bander NH, Smith-Jones PM, Larson SM, Lewis JS. 89Zr-DFO-J591 for ImmunoPET of Prostate-Specific Membrane Antigen Expression In Vivo. The Journal of Nuclear Medicine. 2010; 51:1293–1300. [PubMed: 20660376]
19. Keberle H. The Biochemistry of Desferrioxamine and its Relation to Iron Metabolism. Annals of the New York Academy of Sciences. 1964; 119:758–768. [PubMed: 14219455]
20. Baroncelli F, Grossi G. The complexing power of hydroxamic acids and its effect on the behaviour of organic extractants in the reprocessing of irradiated fuels--I the complexes between benzohydroxamic acid and zirconium, iron (III) and uranium (VI). Journal of Inorganic and Nuclear Chemistry. 1965; 27:1085–1092.
21. Takagai Y, Takahashi A, Yamaguchi H, Kubota T, Igarashi S. Adsorption behaviors of high-valence metal ions on desferrioxamine B immobilization nylon 6,6 chelate fiber under highly acidic conditions. Journal of Colloid and Interface Science. 2007; 313:359–362. [PubMed: 17442331]
22. Perk LR, Visser OJ, Stigter-van Walsum M, Vosjan MJ, Visser GW, Zijlstra JM, Huijgens PC, van Dongen GA. Preparation and evaluation of (89)Zr-Zevalin for monitoring of (90)Y-Zevalin biodistribution with positron emission tomography. Eur J Nucl Med Mol Imaging. 2006; 33:1337–1345. [PubMed: 16832633]

23. Herscheid JD, Hoekstra A, Vos CM. N-Succinyldesferrioxamine B: a potential radiopharmaceutical for assessing renal function. Eur J Nucl Med. 1984; 9:508–510. [PubMed: 6549165]
24. Tinianow JN, Gill HS, Ogasawara A, Flores JE, Vanderbilt AN, Luis E, Vandlen R, Darwish M, Junutula JR, Williams SP, Marik J. Site-specifically 89Zr-labeled monoclonal antibodies for ImmunoPET. Nucl Med Biol. 2010; 37:289–297. [PubMed: 20346868]
25. Meijs WE, Haisma HJ, Van der Schors R, Wijbrandts R, Van den Oever K, Klok RP, Pinedo HM, Herscheid JD. A facile method for the labeling of proteins with zirconium isotopes. Nucl Med Biol. 1996; 23:439–448. [PubMed: 8832698]
26. Perk LR, Visser GW, Vosjan MJ, Stigter-van Walsum M, Tijink BM, Leemans CR, van Dongen GA. (89)Zr as a PET surrogate radioisotope for scouting biodistribution of the therapeutic radiometals (90)Y and (177)Lu in tumor-bearing nude mice after coupling to the internalizing antibody cetuximab. J Nucl Med. 2005; 46:1898–1906. [PubMed: 16269605]
27. Selwyn R, Nickles RJ, Thomadsen BR, DeWard LA, Micka JA. A new internal pair production branching ratio of 90Y: the development of a non-destructive assay for 90Y and 90Sr. Applied Radiation and Isotopes. 2007; 65:318–327. [PubMed: 17045483]
28. Aerts HJWL, Dubois L, Perk L, Vermaelen P, van Dongen GAMS, Wouters BG, Lambin P. Disparity Between In Vivo EGFR Expression and 89Zr-Labeled Cetuximab Uptake Assessed with PET. The Journal of Nuclear Medicine. 2009; 50:123–131. [PubMed: 19091906]
29. Nagengast WB, de Vries EG, Hospers GA, Mulder NH, de Jong JR, Hollema H, Brouwers AH, van Dongen GA, Perk LR, Lub-de Hooge MN. In Vivo VEGF Imaging with Radiolabeled Bevacizumab in a Human Ovarian Tumor Xenograft. The Journal of Nuclear Medicine. 2007; 48:1313–1319. [PubMed: 17631557]
30. Nagengast WB, de Korte MA, Oude Munnink TH, Timmer-Bosscha H, den Dunnen WF, Hollema H, de Jong JR, Jensen MR, Quadt C, Garcia-Echeverria C, van Dongen GAMS, Lub-de Hooge MN, Schroder CP, de Vries EGE. 89Zr-Bevacizumab PET of Early Antiangiogenic Tumor Response to Treatment with HSP90 Inhibitor NVP-AUY922. The Journal of Nuclear Medicine. 2010; 51:761–767. [PubMed: 20395337]
31. Brouwers A, Verel I, Van Eerd J, Visser G, Steffens M, Oosterwijk E, Corstens F, Oyen W, Van Dongen G, Boerman O. PET radioimmunoscintigraphy of renal cell cancer using 89Zr-labeled cG250 monoclonal antibody in nude rats. Cancer Biother Radiopharm. 2004; 19:155–163. [PubMed: 15186595]
32. Perk L, Stigter-van Walsum M, Visser G, Kloet R, Vosjan M, Leemans C, Giaccone G, Albano R, Comoglio P, van Dongen G. Quantitative PET imaging of Met-expressing human cancer xenografts with ^{89}Zr-labelled monoclonal antibody DN30. European Journal of Nuclear Medicine and Molecular Imaging. 2008; 35:1857–1867. [PubMed: 18491091]
33. Holland JP, Caldas-Lopes E, Divilov V, Longo VA, Taldone T, Zatorska D, Chiosis G, Lewis JS. Measuring the Pharmacodynamic Effects of a Novel Hsp90 Inhibitor on HER2/*neu* Expression in Mice Using ^{89}Zr-DFO-Trastuzumab. PLoS ONE. 2010; 5:e8859. [PubMed: 20111600]
34. Oude Munnink TH, Korte MAd, Nagengast WB, Timmer-Bosscha H, Schröder CP, Jong JRd, Dongen GAMSv, Jensen MR, Quadt C, Hooge MNL-d, Vries EGEd. 89Zr-trastuzumab PET visualises HER2 downregulation by the HSP90 inhibitor NVP-AUY922 in a human tumour xenograft. European Journal of Cancer. 2010; 46:678–684. [PubMed: 20036116]
35. Heskamp S, van Laarhoven H, van der Graaf W, Molkenboer-Kuenen J, Oyen W, Boerman O. ImmunoPET and immunoSPECT imaging of IGF-1R expression with radiolabeled R1507. Society of Nuclear Medicine Annual Meeting Abstracts. 2010; 51:397.
36. Borjesson PKE, Jauw YWS, Boellaard R, de Bree R, Comans EFI, Roos JC, Castelijns JA, Vosjan MJWD, Kummer JA, Leemans CR, Lammertsma AA, van Dongen GAMS. Performance of Immuno,ÄìPositron Emission Tomography with Zirconium-89-Labeled Chimeric Monoclonal Antibody U36 in the Detection of Lymph Node Metastases in Head and Neck Cancer Patients. Clinical Cancer Research. 2006; 12:2133–2140. [PubMed: 16609026]
37. Borjesson PKE, Jauw YWS, de Bree R, Roos JC, Castelijns JA, Leemans CR, van Dongen GAMS, Boellaard R. Radiation Dosimetry of 89Zr-Labeled Chimeric Monoclonal Antibody U36 as Used for Immuno-PET in Head and Neck Cancer Patients. The Journal of Nuclear Medicine. 2009; 50:1828–1836. [PubMed: 19837762]

38. Dijkers EC, Oude Munnink TH, Kosterink JG, Brouwers AH, Jager PL, de Jong JR, van Dongen GA, Schroder CP, Lub-de Hooge MN, de Vries EG. Biodistribution of 89Zr-trastuzumab and PET Imaging of HER2-Positive Lesions in Patients With Metastatic Breast Cancer. Clin Pharmacol Ther. 2010; 87:586–592. [PubMed: 20357763]

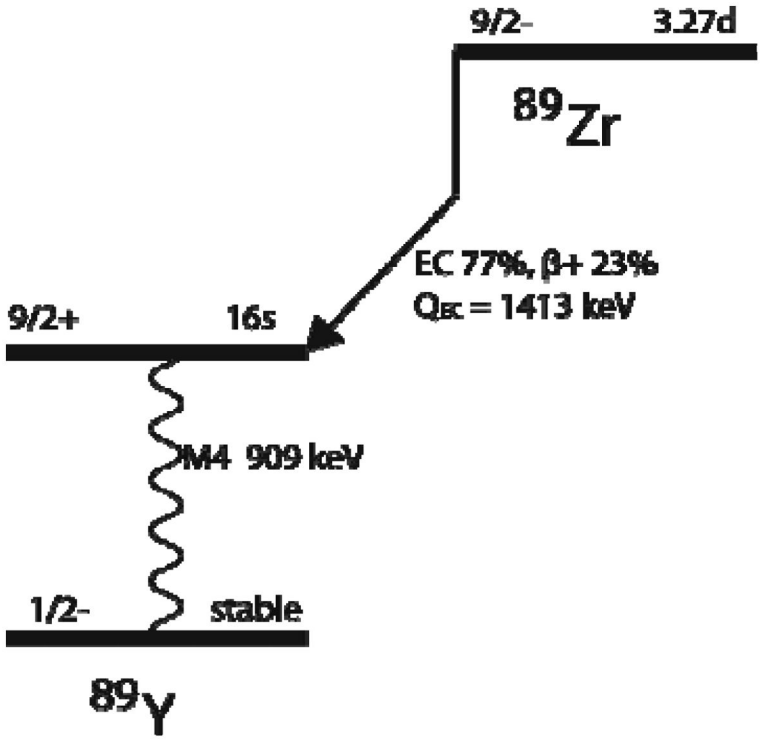

Figure 1.
A simplified ^{89}Zr decay scheme

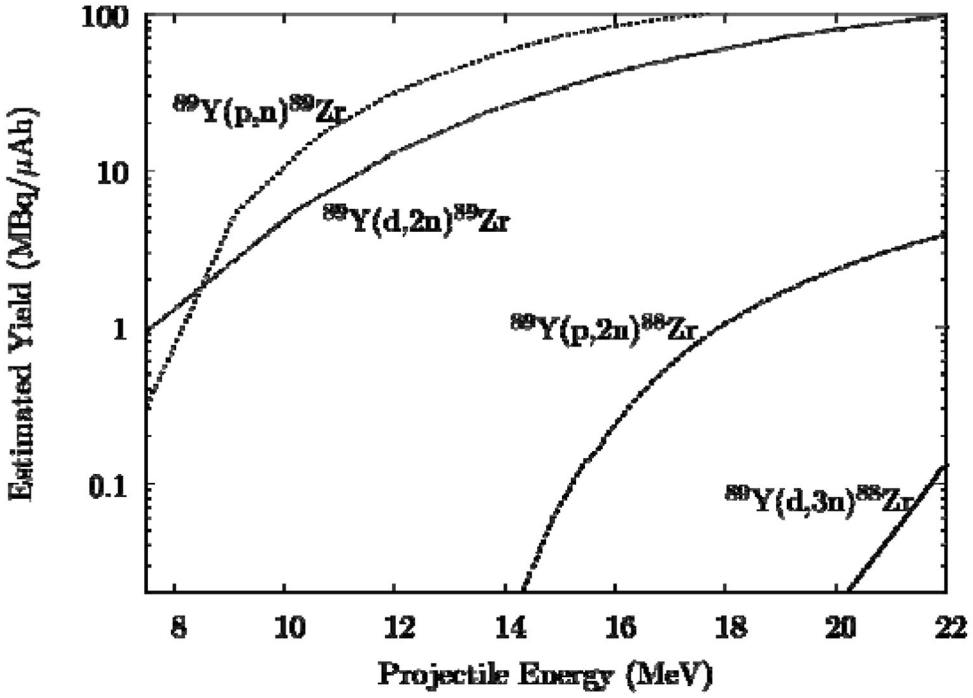

Figure 2.

Estimated thick target yields for short irradiations of yttrium metal. The plot is adapted from [11], using additional cross-section data from [13,14].

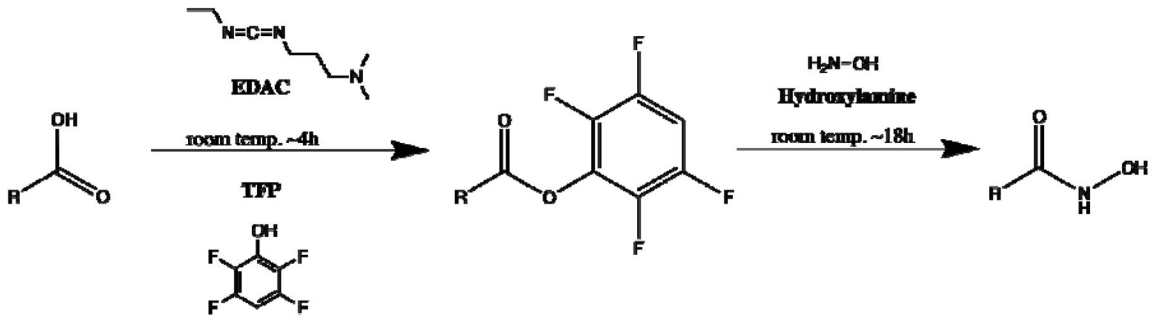

Figure 3.

The mechanism for creating the hydroxamic resin. In this figure, R represents a connection back to the resin.

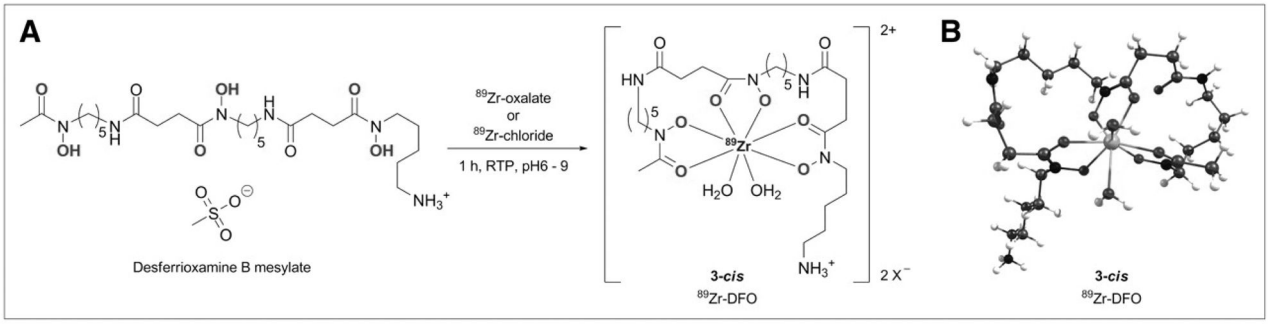

Figure 4.

The structure of Desferrioxamine B. The hydroxamic groups participate in metal chelation while the terminal amine is used to functionalize the Df for linkage to mAbs. Taken from reference [18]. (A) depicts the chelation reaction, while (B) shows the stable geometry.

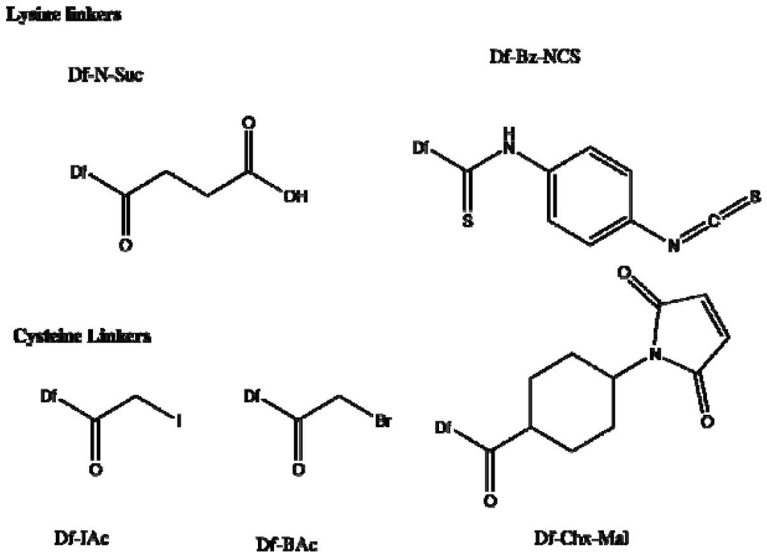

Figure 5.
The reactive modifications to Df. Adapted from reference [24].